

## A SIMPLE APPROACH TOWARDS TUNING MORPHOLOGY OF MICROCRYSTALLINE CELLULOSE

VINAYA B. GHODAKE,<sup>\*,\*\*</sup> RUPESH A. KHARE<sup>\*</sup> and SHASHANK T. MHASKE<sup>\*\*</sup>

<sup>\*</sup>*Pulp and Fibre Innovation Centre (Grasim Industries), Aditya Birla Science and Technology Centre, MIDC Talaja-410208, Tal Panvel, Maharashtra, India*

<sup>\*\*</sup>*Department of Polymer Science and Engineering, Institute of Chemical Technology, N. Parekh Marg, Matunga – 410019, Mumbai, India*

✉ *Corresponding author: S. T. Mhaske, st.mhaske@ictmumbai.edu.in*

Received June 28, 2022

Microcrystalline cellulose (MCC) is a purified cellulose derivative. It is a white, highly oriented form of cellulose most commonly used in food, cosmetic, and pharmaceutical industries due to its advantageous properties of high crystallinity, large surface area, good compressibility *etc.* MCC is a high value added material that is widely used in pharmaceutical companies. For such applications, a large surface area of MCC is important. In this study, MCC was prepared from cellulosic fibres with a specific cross-section, *i.e.* trilobal, to produce trilobal microcrystalline cellulose (TMCC), which has a large surface area. This MCC is produced by a simple acid hydrolysis process. The process parameters in the production of MCC were optimised to maintain the cross-sectional shape of the fibres, even after conversion to MCC. The obtained MCC was characterized by various analytical techniques, such as Fourier transform-infrared spectroscopy (FTIR), thermogravimetric analysis (TGA), B.E.T surface and X-ray diffraction (XRD) analyses. The cross and longitudinal morphology of the produced MCC was confirmed by scanning electron microscopy (SEM). The study shows that strong hydrolysis conditions, such as higher temperatures of 50 to 55 °C, lead to distortion of the cross-section, while lower reaction temperatures, *i.e.* 25 to 30 °C, help maintain a trilobal morphology. It was also found that the thermal stability of TMCC is higher, compared to that of regular MCC. The maximum decomposition temperature of TMCC was 304 °C, while it was 270 °C for regular MCC. The crystallinity index of all MCC was in a similar range. In addition, the water retention value (WRV) of TMCC was higher than that of circular MCC, indicating effectiveness of the increased surface area. The maximum WRV for MCC and TMCC was 66 and 85%, respectively.

**Keywords:** cellulose fibre, morphology, hydrolysis, water retention value

### INTRODUCTION

Cellulose is the most abundant, renewable resource, which is also biodegradable, biocompatible, and easy to modify.<sup>1,2,3</sup> It is a linear homopolymer consisting of 1-4 linked  $\beta$ -D-glucose units, which form long elemental fibrils linked by hydrogen bonding to form microfibrils.<sup>4</sup> The use of cellulosic materials is gaining importance due to their properties and sustainable applications. Therefore, it is becoming increasingly important to accelerate the transition from traditional to environmentally friendly materials, to support the transition to equitable, sustainable societies without fossil fuels.<sup>5</sup> This can be achieved by using different

types of cellulosic materials, such as nanocrystalline cellulose,<sup>6</sup> cellulose nanowhiskers,<sup>7</sup> microfibrillated cellulose<sup>8</sup> and microcrystalline cellulose.<sup>9</sup> These forms of cellulose obtained by various methods present high surface area, aspect ratio, thermal stability and good barrier properties, which makes them promising for specific applications.<sup>10</sup>

Researchers have reported the synthesis of MCC from various feedstocks, such as kenaf fibers,<sup>11</sup> rice husk,<sup>12</sup> cotton linter,<sup>13</sup> sawdust,<sup>14</sup> rice straw,<sup>15</sup> oil palm empty fruit bunch,<sup>16</sup> groundnut shells,<sup>17</sup> corn cobs,<sup>18</sup> sisal fibers,<sup>19</sup> cotton rags<sup>20</sup> *etc.* Currently, many researchers are investigating new renewable

cellulosic sources based on wastes generated in industrial processing; e.g. carpenter waste in sawmills. These wood-based raw materials consist of hemicelluloses and lignin, along with cellulose, and these two components need to be separated before such sawmill wastes can be used to synthesise MCC.<sup>21</sup> An alternative source for obtaining cellulose can be the fibres from date palm fronds. Firstly, these date palm fibres are delignified with various reagents, such as acidified NaClO<sub>2</sub>, by total chlorine free (TCF) processes or their combination. After delignification, MCC is produced by acid hydrolysis.<sup>22</sup> Also, the possibility of synthesizing MCC from giant reed has been investigated.<sup>23</sup> Giant reed must also be delignified before MCC synthesis. Actually, all identified plant sources need to be pretreated in order to remove low molecular weight short chains, such as hemicelluloses, lignin and any resins or impurities. MCC can then be synthesized by various techniques, including chemical processes, reactive extrusion, high-pressure homogenization, and steam explosion.<sup>24</sup>

MCC is a fine, odourless, white, crystalline powder with important properties, such as non-toxicity, biocompatibility, biodegradability, high mechanical strength, and low density.<sup>25,26</sup> Due to these properties, it has attracted much attention in recent decades and has been used in various industries. In particular, it has been used in the food, cosmetic and medical industries as a binder and filler in foods, medical tablets,<sup>27</sup> *etc.* In addition, it has been used as a reinforcing agent in the development of polymer composites.<sup>28</sup> MCC is also used as a suspension stabilizer, water retention agent, viscosity regulator, and emulsifier in pastes and creams.<sup>29,30</sup> Recent studies have focused on the development of smart functional materials based on MCC, such as humidity sensor transformers,<sup>31</sup> hydrogels<sup>32</sup> and composite films with dielectric properties.<sup>33</sup> Considering these multiple potential applications, as well as the importance of surface area for specific applications, it is of interest to investigate the possibility of producing MCC with different shape in cross-section to increase the surface area.

Literature describes that the most common morphology of MCC can be of two types: rod-shaped<sup>34</sup> and spherical.<sup>35</sup> The morphology of MCC is determined by its cellulose source, and a few

studies have mentioned the formation of aggregates of cellulose particles due to treatment conditions,<sup>36</sup> for example, rod-shaped morphology of MCC obtained from bamboo fibre.<sup>37</sup> Spherical or granular morphology of MCC can be prepared by using processes such as granulation or spheronization.<sup>38</sup>

In this research, we present a top-down approach which allows preparing MCC with the desired cross-section shape, starting from cellulosic fibres of predefined cross-section.

## EXPERIMENTAL

### Material

Cellulosic fibres with specified morphology, such as trilobal and circular (regular) viscose fibres, were prepared at the Pulp and Fibre Innovation Center, India. Caustic soda (NaOH), carbon disulphide (CS<sub>2</sub>), concentrated sulphuric acid (H<sub>2</sub>SO<sub>4</sub>) (98%), zinc sulphate (ZnSO<sub>4</sub>), hydrogen peroxide (H<sub>2</sub>O<sub>2</sub>), sodium carbonate (Na<sub>2</sub>CO<sub>3</sub>) and acetic acid were obtained from Merck, India.

### Spinning of circular (regular) and trilobal viscose fibre

A standard viscose dope preparation process consists of multiple steps, like steeping, shredding, aging, xanthation, dissolution, and ripening. Dissolving grade pulp was treated in 18% caustic solution in the steeping process for 20 min, followed by pressing to remove excess alkali from the slurry. Alkaline cellulose, denoted as Alkcell, was shredded to break crumbles. This shredded Alkcell was aged in a maturing drum for 50 min at 50 °C, and subsequently reacted with CS<sub>2</sub> under vacuum to form cellulose xanthate. Cellulose xanthate was dissolved in cold alkaline water to form the viscose dope. Further, the viscose dope was filtered using 35-micron mesh and deaerated to remove air bubbles. The deaerated viscose dope was used for regular viscose fibre spinning. Viscose was spun with a spinneret with 60-micron capillary and 250 holes. The fibres were regenerated into a spin-bath containing: 110-120 g/L of H<sub>2</sub>SO<sub>4</sub>, 10 g/L of ZnSO<sub>4</sub>, and 355 g/L of Na<sub>2</sub>SO<sub>4</sub>. The spin-bath temperature was maintained at 50 °C and stretching at 68% was provided to fibres between the two gadgets. Fibres were collected on a roller. Formed viscose fibres were cut into 38 mm length and washed with dilute acid, alkali and further washed with hot water. The washed fibres were treated with H<sub>2</sub>O<sub>2</sub> for bleaching them, followed by dilute acetic acid for neutralization. Finally, these fibres were dried in an oven at 105 °C for 20 min. A similar process was followed to prepare trilobal fibre using a specialized spinneret with trilobal-shaped capillaries.

### Preparation of microcrystalline cellulose (MCC)

As described in the schematic for MCC preparation in Figure 1, 5 g of each fibre (regular viscose and trilobal) was hydrolysed with 55% H<sub>2</sub>SO<sub>4</sub> in a beaker, keeping the ratio of H<sub>2</sub>SO<sub>4</sub> to fibre as 20:1, at a temperature in the ranges of 25-30 °C, 40-45 °C and 50-55 °C, under stirring. After completing the hydrolysis

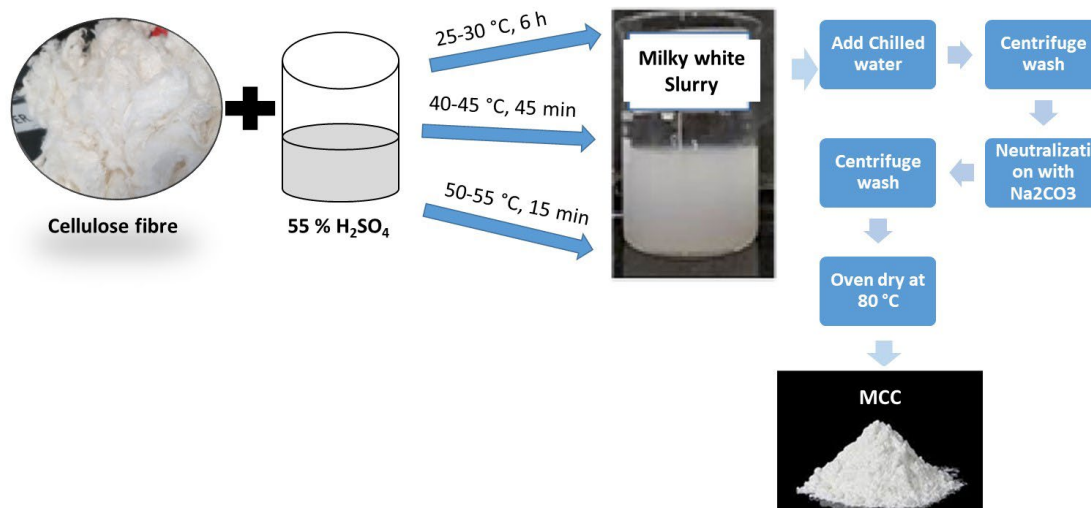


Figure 1: Schematic for MCC preparation

### Identification and characterization of MCC

#### Gel permeation chromatography (GPC)

A GPC (Agilent 1260 Infinity II HT GPC instrument model) was used to determine the molecular weight distribution of pristine fibres and extracted MCC. The samples were dissolved in N,N-dimethyl acetamide (DMAc) and lithium chloride (LiCl) and used for analysis.

#### Optical microscopy

The cross-section of regenerated cellulose fibres was observed under a Carl Zeiss Axio scope A1 optical microscope, in transmittance mode at 100x magnification.

#### Fourier transform infrared (FTIR) spectroscopy

FTIR spectra were recorded on a Shimadzu attenuated total reflection Fourier transform infrared (ATR-FTIR) spectrophotometer to analyse the MCC prepared from different fibre samples. FTIR spectral analysis was performed within the wavelength range of 400-4000 cm<sup>-1</sup> with a resolution of 4 cm<sup>-1</sup> and a total of 45 cumulative scans were taken.

#### X-ray diffraction analysis (XRD)

The XRD patterns for all MCC samples were obtained with an X-ray diffractometer (D8 Advance,

process, the obtained slurry was quenched with ice-cold water and centrifuged. Then, it was washed with water to remove excess acid. Finally, it was neutralized with 1.5 molar Na<sub>2</sub>CO<sub>3</sub> solutions to remove traces of acid and was again washed with water. The obtained MCC powder was dried in an oven at 80 °C for 1 h. This dried MCC was used for further analysis.

Bruker, Germany), using Cu K $\alpha$  radiation at 40 kV and 100 mA. Scattered radiation was detected in the 2 $\theta$  diffraction range of 5–50°. The MCC samples were dried at 80 °C under vacuum and used for XRD analysis. The spectra were recorded for the powder material on a glass slide at a scan rate of 4° min<sup>-1</sup>.

The percent crystallinity index (%CrI) was calculated using the Gaussian model procedure:<sup>39</sup>

$$\% \text{CrI} = \frac{(\text{Icr peak 1} + \text{Icr peak 2} + \text{Icr peak 3} \dots)}{(\text{Icr peak 1} + \text{Icr peak 2} + \text{Icr peak 3} \dots + \text{Inoncr peak})} \times 100 \quad (1)$$

#### Scanning electron microscopy (SEM)

The morphology of MCC in cross-sectional and longitudinal orientation was observed under a Phenom XL (Phenom Pro X, Netherlands) SEM microscope. All samples were gold sputtered to avoid charging during analysis. Samples were illuminated at 10 kV.

#### Thermogravimetric analysis (TGA)

The thermal behaviour of MCC was studied using a simultaneous TGA SDT Q600 (TA Instruments). The samples weighing from 7 to 12 mg were placed in a platinum crucible. The measurements were recorded from 25 °C to 650 °C, at the rate of 10 °C per min under nitrogen. Thermograms were analysed using Universal analysis software.

**BET surface area**

Specific surface area of MCC was determined by adsorption of N<sub>2</sub> at low temperatures (BET technique), by a surface area analyser (Qunatachrome, Nova-1000e).

**Water retention value (WRV)**

0.25 g of MCC was accurately weighed (W<sub>0</sub>), and then transferred into a 250 mL beaker, to which 100 mL of water was added. After the soaking time of 1 h, the MCC was transferred into a specialized glass tube, having a sintered disk at the middle of the tube. A 0.2 μm filter, with a weight denoted as W<sub>1</sub>, was placed in a tube and MCC was poured into it. The tubes were allowed to stand for 30 min. Then, the glass tubes were centrifuged in a plastic tube for 30 min at 3000 rpm to remove excess water. After centrifugation, the glass tubes were removed from the plastic tube and weighed (W<sub>2</sub>). MCC was further dried in an oven at 105 °C for 1 h and cooled in a desiccator for 1 h. The dry weight (W<sub>3</sub>) was noted down. The WRV of MCC was calculated using the formula below:

$$\text{Water retention value (\%)} = \frac{((W_2 - W_1) - W_0)}{W_0} \quad (2)$$

**RESULTS AND DISCUSSION**

Considering emerging applications of MCC in multiple areas, there is a need to find ways to

improve the properties of MCC, for instance, increase their surface area. A simple approach for this is to start with a precursor material that has larger surface area and find a method to retain it even after conversion to MCC. In this study, we adopted such a route using viscose fibres of different cross-section, *viz.* circular (regular) viscose fibre and trilobal shaped viscose fibre, to produce regular MCC and trilobal MCC (T-MCC), respectively.

The spinning of these different types of fibres was described in the experimental part of this paper. The characterization of the fibres was carried out by a number of techniques. The morphology of the spun fibre sample, confirmed through optical microscopy, is depicted in Figure 2. The morphology of regular viscose fibre shows circular and serrated shape, as shown in Figure 2 (A) and that of the fibre formed with a specialized spinneret shows trilobal shape Figure 2 (B).

Table 1 describes the characteristic properties of the precursor cellulose fibre used for the synthesis of MCC.

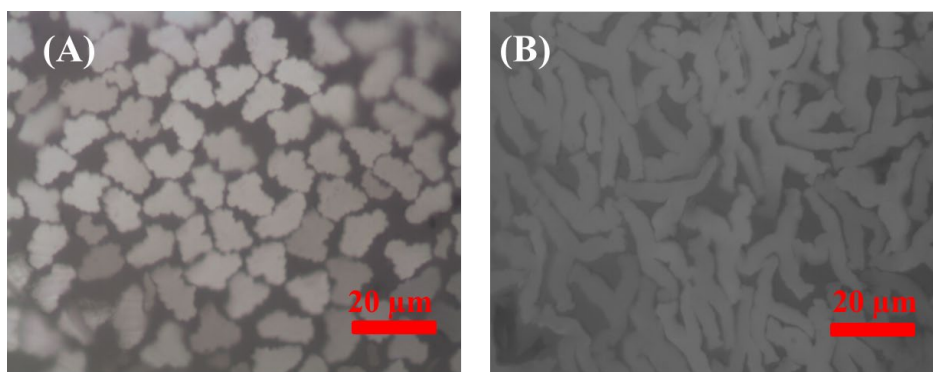


Figure 2: Optical images of prepared (A) viscose fibre, and (B) trilobal fibre

Table 1  
Characteristic properties of precursor cellulose fibres

Properties	Viscose fibre	Trilobal fibre
Viscosity (mL/g)	178	175
DP	223	219
Crystallinity (%)	36	38
Degradation temperature	294	301
Weight loss (%)	86.4	87
WRV (%)	66	73

Table 2  
Hydrolysis treatment conditions to form MCC from different precursor fibres

Sample	Morphology of base fibres	H <sub>2</sub> SO <sub>4</sub> , %	Time	Yield, %
MCC-1	Serrated	55	6 h	77.3
MCC-2			45 min	74.9
MCC-3			15 min	71.6
TMCC-1	Trilobal		6 h	75.3
TMCC-2			45 min	76.0
TMCC-3			15 min	74.4

Viscosity is an important physicochemical property of fibre. In this case, the fibre was dissolved in cupraethylene diamine (CED solution) and the response to the flow of the solution was measured at 20 °C in the capillary viscometer. It is the measurement of the resistance to flow of a fluid in a capillary, which expresses the molecular fraction. This is correlated with the degree of polymerization. The result showed that both viscose and trilobal fibre have comparable viscosity – of 178 and 175 mL/g, respectively, and the corresponding degree of polymerization was around 223 and 219, respectively. Other properties, such as crystallinity and thermal stability, were comparable. However, the WRV of viscose fibre was 66% and that of trilobal fibre – of 73%. Hence, the cellulose fibres were converted to microcrystalline form by the acid hydrolysis method. The precursor cellulosic fibres were treated under different hydrolysis conditions, while maintaining the concentration of sulphuric acid at 55 wt%, to ensure hydrolysis time and temperature were varied to alter the kinetics of hydrolysis, as noted in Table 2. Further, the yield of MCC was observed to be similar for all types of precursor fibres and hydrolysis conditions. Thus, it further corroborates the fact that optimization of hydrolysis conditions only alters the kinetics and not the extent of hydrolysis itself.

### Molecular weight distribution

The GPC analysis provides information on molecular weight distribution (MWD), which including the number average (Mn) and weight average (Mw) molecular weight. Along with this, the polydispersity index (PDI) is an important parameter for the determination of heterogenic distribution of cellulose chains<sup>40</sup> and it is calculated by Mw/Mn. The results of GPC analysis greatly depend on the processing of cellulose, such as dissolution, conditioning, treatment *etc.* In this study, the number (Mn) and weight (Mw) average molecular weight distribution of pristine fibre and its MCC were evaluated. The acid hydrolysis for the conversion of fibre into MCC led to reduction in both Mn and Mw, as shown in Table 3.

Figure 3 shows the MWD of fibre and MCC. The MWD is observed to be narrow for acid hydrolysed MCC, as compared to the raw fibre. This can be due to chain breaking during hydrolysis, resulting in a decrease in the molecular weight of MCC.<sup>36</sup> It is observed that the hydrolysis of cellulose with a strong acid, such as H<sub>2</sub>SO<sub>4</sub>, results in the degradation of cellulose and further removal of soluble small molecular weight components, leading to narrowing of MWD.

Table 3  
Molecular weight distribution of fibres and MCC

Sample	Mn (g/mol)	Mw (g/mol)	PDI
Viscose fibre	26818	94130	3.51
Trilobal fibre	33866	130364	3.85
VMCC	4793	9978	2.08
TMCC	5315	15118	2.84

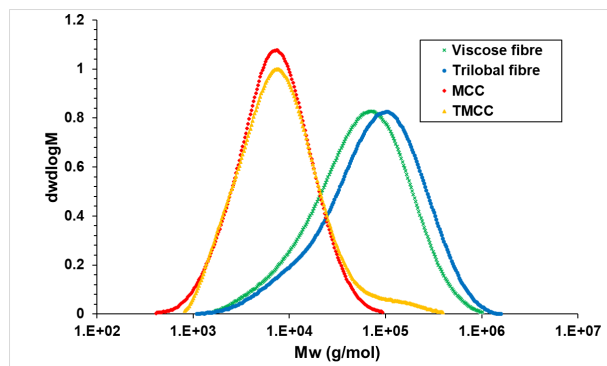


Figure 3: MWD of Fibre and MCC

### Microscopic analysis for understanding morphological changes

The morphology of MCC obtained from regular and trilobal shaped precursor fibres was evaluated through SEM, as depicted in Figures 4 and 5, for cross-section and longitudinal views, respectively. Cellulosic fibres with different morphology were subjected to acid hydrolysis to convert them into MCC, while retaining their original morphology. Figure 4 (A)–(C) depicts the cross-section of MCC prepared from regular viscose fibre. These microscopic images reveal the serrated and oval cross-section of MCC, similar to their precursor fibres. Further, Figure 4 (D)–(F) illustrate the cross-section of TMCC, *i.e.* MCC prepared from trilobal cellulosic fibre as precursor under different

hydrolysis conditions. As observed from the cross-section, it is evident that lower hydrolysis temperature, that is 25–30 °C, allows retaining the trilobal shape in MCC, whereas higher hydrolysis temperature (50–55 °C) results in distortion of the trilobal morphology. MCC prepared from trilobal fibres at higher hydrolysis temperature show splitting of these lobes into individual fragments.

Figure 5 presents the longitudinal section of MCC prepared from viscose fibres with different cross-section, at varying hydrolysis conditions as stated above. Figure 5 (A)–(C) shows the longitudinal surface of MCC obtained from regular viscose fibre and depicts ridges over the length of MCC, which correspond to serrations observed in the cross-section of these fibres.

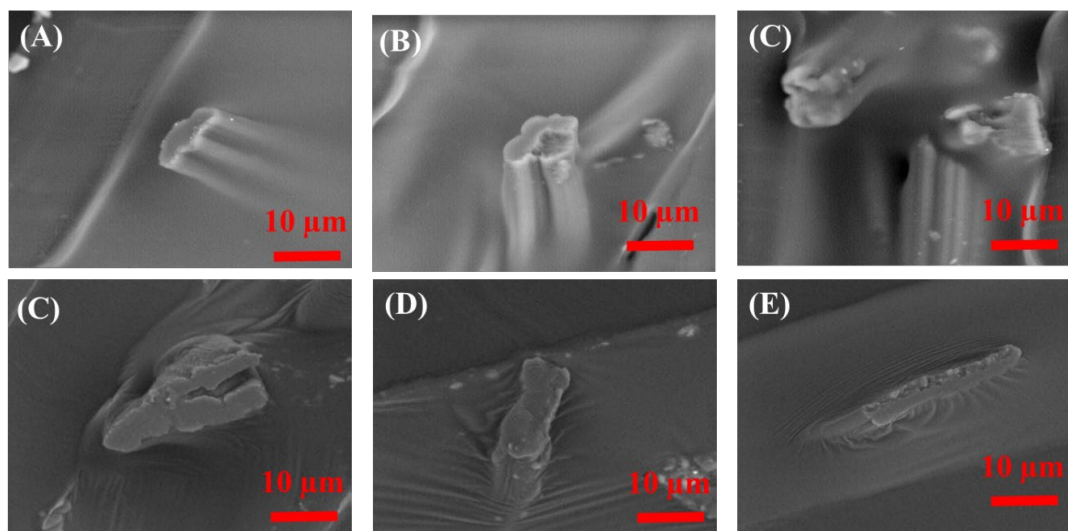


Figure 4: SEM images of the cross-section of (A) MCC-1, (B) MCC-2, (C) MCC-3, and (D) TMCC-1, (E) TMCC-2 and (F) TMCC-3

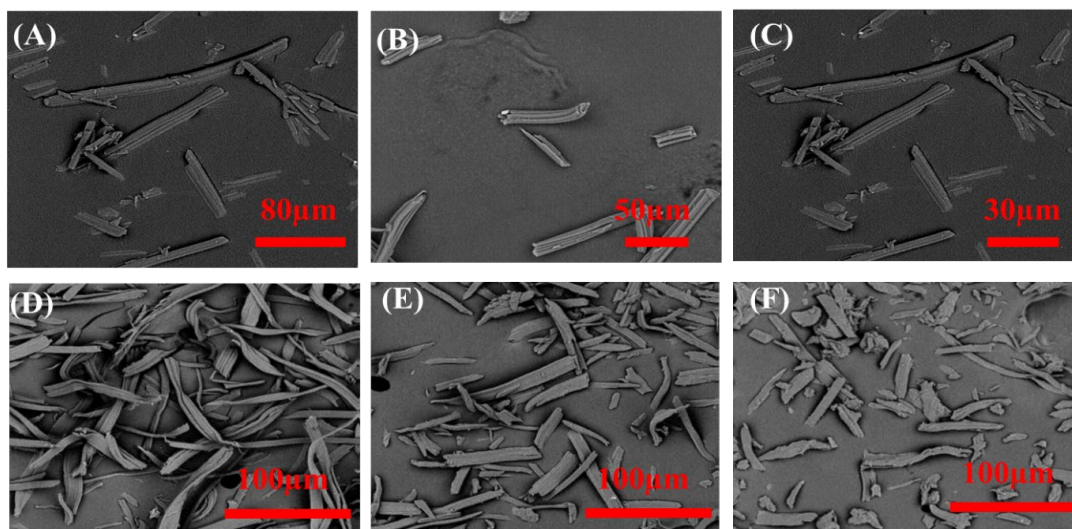


Figure 5: SEM images of the longitudinal surface morphology of (A) MCC-1, (B) MCC-2, (C) MCC-3, and (D) TMCC-1, (E) TMCC-2 and (F) TMCC-3

Figure 5 (D)–(F) depicts the longitudinal view for TMCC prepared from trilobal viscose fibres. Interestingly, progressively harsher conditions of hydrolysis result in a decrease in the length or aspect ratio of MCC for all types of precursors.

#### Influence of hydrolysis on chemical structure

Figure 6 illustrates the FTIR spectra for regular MCC and trilobal MCC. The cellulose peak shows changes in intensity for MCC prepared from different cellulosic fibres. The observed peaks in the wavelength range of  $3660\text{--}2900\text{ cm}^{-1}$  are characteristic of the stretching vibration of O-H and C-H bonds in polysaccharides. The broad peak at  $3331\text{ cm}^{-1}$  is characteristic of the stretching vibration of the hydroxyl group in polysaccharides. The band at  $2894\text{ cm}^{-1}$  is attributed to the -CH stretching vibration of all hydrocarbon constituents in polysaccharides.<sup>41</sup> Typical bands assigned to cellulose were observed in the region of  $1630\text{--}900\text{ cm}^{-1}$ . The peaks located at  $1633\text{ cm}^{-1}$  correspond to the vibration of water molecules absorbed in cellulose.<sup>41</sup> The absorption bands at 1428, 1367, 1334, 1027 and  $896\text{ cm}^{-1}$  belong to the stretching and bending vibrations of -CH<sub>2</sub> and -CH, -OH and C-O bonds in cellulose. The band around  $1420\text{--}1430\text{ cm}^{-1}$  is associated with the amount of the crystalline structure of cellulose, while the peak at  $897\text{ cm}^{-1}$  is assigned to the amorphous region in cellulose.<sup>42</sup>

#### Crystallinity index of MCC after drying

Figure 7 shows the XRD patterns for all the prepared MCC samples. The crystallinity index of acid hydrolysed MCC showed peaks at 12.5 (1-1 0), 20.1 (110), and 22.1 (200), indicating the formation of MCC. Acid hydrolysis aims to reduce the amorphous regions between microfibrils, while the crystalline segments remain intact because the kinetics of hydrolysis in the amorphous region is faster than in the crystalline region, due to its higher permeability.<sup>42</sup> Therefore, the conversions of cellulose I from the original to cellulose II were successfully achieved.<sup>43</sup> A similar diffraction pattern was observed for all MCC samples. Further, it is worth mentioning that all MCC indicated the presence of split peaks at  $2\theta$  value of  $20\text{--}23^\circ$ , indicating the conversion of the native cellulose structure into cellulose II form.

The crystallinity index calculated by the Gaussian modal curve (eq. 1) shows high crystallinity for acid hydrolysed MCC. This describes the benefit of reduction of the amorphous region in cellulose due to acid hydrolysis and the selective retention of the crystalline region. Table 2 describes the % crystallinity index of the prepared MCC. It should be noted that the TMCC formed from trilobal cellulosic fibre showed a similar crystallinity index, except for TMCC-3 prepared at  $50\text{ }^\circ\text{C}$ , which is 64%. Such a reduction is

presumably caused by the higher degradation at a high reaction temperature, which affected even the

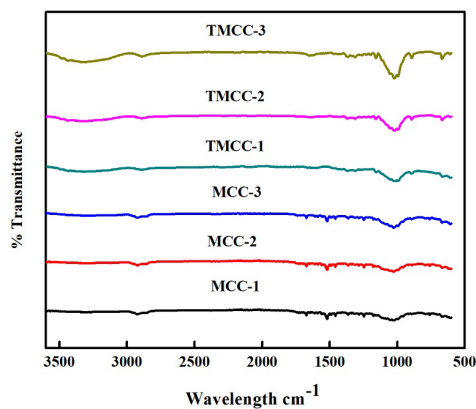


Figure 6: FTIR spectra of MCC

crystalline region.

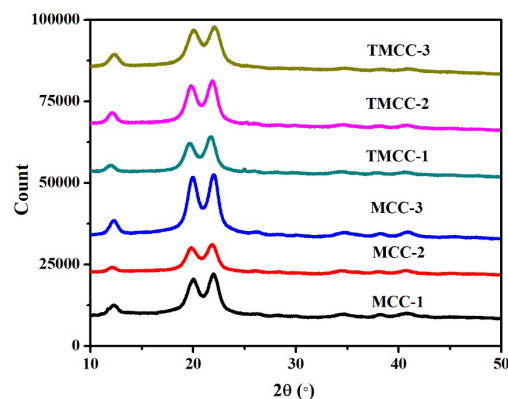


Figure 7: XRD patterns of MCC

Table 4  
Crystallinity index of MCC

Sample	Crystallinity index (%)
MCC-1	60
MCC-2	62
MCC-3	61.6
TMCC-1	68.4
TMCC-2	68.2
TMCC-3	64.4

### Thermogravimetric analysis

The thermal stability of any material is a crucial parameter for its use in any application. The TGA curves of MCC and TMCC are shown in Figure 8. The curves indicate that the degradation occurs in a two-stage pattern. The first weight loss stage at 70 °C is due to the evaporation of water molecules,<sup>44,45</sup> and the second, in the temperature range of 284-305 °C, indicates the onset of degradation. The major decomposition temperature peak for TMCC is observed at 270 °C. This could be due to the high degree of molecular ordering in TMCC, which requires high heat energy for thermal degradation.<sup>11</sup> Table 5 lists the thermal analysis results. As observed from the data, the residue remaining at the end of degradation for regular MCC was higher (20%) than for TMCC samples, even though it showed an early onset of degradation.

### BET surface area

The BET surface area of MCC has been studied and reported in the literature,<sup>46</sup> as well as that of commercially available MCC (Avicel PH-102).<sup>47</sup> The specific surface area and the pore volume mentioned for MCC are 1.32 m<sup>2</sup>/g and 0.02405 cm<sup>3</sup>/g, respectively.<sup>48</sup> Table 3 lists the results of BET surface area analysis for the different MCC prepared in our study. As observed from the data, the surface area and the pore volume for MCC prepared using regular viscose fibre were too low to be determined precisely. TMCC clearly shows higher surface area, as expected. However, no significant difference in surface area was observed by further optimization of the hydrolysis conditions. Since there are no voids present in the structure of TMCC, the pore size was observed to not change with hydrolysis conditions.

### Water retention value (WRV)

Water absorption and retention for any substance is an important property of materials, and often, it can be tuned by changing the surface area according to the required application. Water retention value (WRV) in particular can be influenced strongly by

altering the morphology of the material. As illustrated in Figure 9, a significant difference in WRV can be observed for viscose and trilobal fibres, which is 66% and 73%, respectively, based on their morphology.

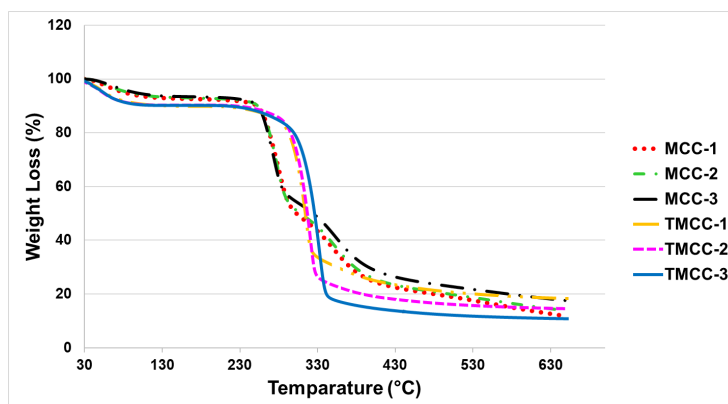


Figure 8: Thermogravimetric analysis of MCC

Table 5  
Thermal analysis and BET surface area

Samples	T (°C) <sup>a</sup>	Weight loss (%)	Char residue (%)	Surface area (m <sup>2</sup> /g)	Pore volume (cc/g)	Pore size (Å)
MCC-1	270.3	84.4	11.8	ND	ND	ND
MCC-2	272.1	87.2	13.8	ND	ND	ND
MCC-3	269.9	97.6	17.6	ND	ND	ND
TMCC-1	290.0	81.6	18.4	2.82	0.00107	4.73
TMCC-2	295.5	85.4	14.6	2.25	0.00105	4.73
TMCC-3	304.0	89.1	10.9	3.94	0.00151	4.73

a: Onset of degradation; ND: Not detected

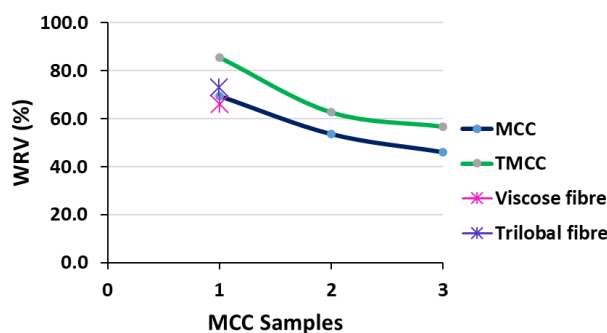


Figure 9: Water retention value (WRV) of MCC

Similarly, the effect of morphology on WRV could be observed for MCC. As observed in Figure 9, the WRV of 85% observed in TMCC represented the highest level of WRV, followed by MCC (66%) prepared from regular viscose fibres. Further, with

increasing hydrolysis temperature, a reduction in WRV is observed for all types of MCC. Thus, the reduction is likely due to shortening of MCC (reduced aspect ratio), as observed earlier from SEM analysis (Fig. 4).

Overall, this study provides a simple approach towards tuning the morphology and surface area of MCC by adopting a top-down approach of selecting a suitable precursor material and adjusting the hydrolysis conditions. It further opens up the opportunity to exploit such higher surface area in specific applications, requiring water retention or the possibility of increasing the grafting density of different functional groups on the surface of MCC.

## CONCLUSION

Cellulosic fibres of different morphology, namely circular and trilobal fibres, were subjected to acid hydrolysis under different conditions to convert into MCC, with the aim of retaining the cross-sectional morphology of initial fibres and achieving higher surface area. These MCC were characterized using several techniques. TMCC presented higher surface area than circular MCC. In addition, high crystallinity index and high thermal stability could be obtained by optimization of the time and temperature of the hydrolysis of cellulosic fibres. The water retention value was observed to be governed by such hydrolysis conditions, verifying the modified surface area and also confirming the microscopic analysis of morphology. The findings demonstrate a simple way to increase the surface area of MCC for important applications, involving grafting of different chemical molecules onto the surface of MCC.

**ACKNOWLEDGEMENT:** The authors duly acknowledge the support of Pulp and Fibre Innovation Centre (Grasim Industries) for providing the required resources, and Aditya Birla Science and Technology Centre for offering analytical facilities.

## REFERENCES

- <sup>1</sup> L. Ding, Y. Jiang, B. Wang, Y. Li and Z. Mao *et al.*, *Cellulose*, **25**, 7369 (2018), <https://doi.org/10.1007/s10570-018-2068-9>
- <sup>2</sup> Y. Zheng, Z. Fu, D. Li and M. Wu, *Materials*, **11**, 1 (2018), <https://doi.org/10.3390/ma11071057>
- <sup>3</sup> S. Wang, A. Lu and L. Zhang, *Progress Polym. Sci.*, **53**, 169 (2016), <https://doi.org/10.1016/j.progpolymsci.2015.07.003>
- <sup>4</sup> R. J. Moon, A. Martini, J. Nairn, J. Simonsen and J. Youngblood, *Chem. Soc. Rev.*, **40**, 3941 (2011), <http://dx.doi.org/10.1039/c0cs00108b>
- <sup>5</sup> C. Ingrao, J. Bacenetti, A. Bezama, V. Blok and J. Geldermann, *J. Clean. Prod.*, **117**, 4 (2016), <https://doi.org/10.1016/j.jclepro.2015.12.066>
- <sup>6</sup> J. N. Putro, S. P. Santoso, F. E. Soetaredjo, S. Ismadji and Y. H. Ju, *Environ. Nanotechnol. Monitor. Manag.*, **12**, 100260 (2019), <https://doi.org/10.1016/j.enmm.2019.100260>
- <sup>7</sup> S. J. Eichhorn, *Soft Matter*, **7**, 303 (2011), <https://doi.org/10.1039/c0sm00142b>
- <sup>8</sup> A. M. Adel, A. A. El-Gendy, M. A. Diab, R. E. Abou-Zeid, W. K. El-Zawawy *et al.*, *Ind. Crop. Prod.*, **93**, 161 (2016), <https://doi.org/10.1016/j.indcrop.2016.04.043>
- <sup>9</sup> H. Suryadi, Sutriyo, M. Angeline and M. W. Murti, *J. Young Pharmacists*, **10**, 87 (2018), <https://doi.org/10.5530/jyp.2018.2s.17>
- <sup>10</sup> A. Dufresne, *Curr. For. Reports*, **5**, 76 (2019), <https://doi.org/10.1007/s40725-019-00088-1>
- <sup>11</sup> D. Trache, M. H. Hussin, C. T. Hui Chuin, S. Sabar, M. R. Fazita *et al.*, *Int. J. Biol. Macromol.*, **93**, 789 (2016), <https://doi.org/10.1016/j.ijbiomac.2016.09.056>
- <sup>12</sup> Z. Ahmad, N. N. Roziaizan, R. Rahman, A. F. Mohamad and W. I. Wan Ismail, *MATEC Web of Conferences*, **47**, 1 (2016), <https://doi.org/10.1051/mateconf/20164705013>
- <sup>13</sup> M. A. Abd-Allah Nada, M. Y. El-Kady, E. S. Abd El-Sayad and F. M. Amina, *BioResources*, **4**, 1359 (2009), <https://doi.org/10.15376/BIORES.4.4.1359-1371>
- <sup>14</sup> P. Chuayplod and D. Aht-Ong, *J. Metals Mater. Minerals*, **28**, 106 (2018), <https://doi.org/10.14456/jmmm.2018.33>
- <sup>15</sup> K. M. Chin, S. S. Ting, O. H. Lin and W. T. Owi, *AIP Conf. Proc.*, **1865**, 040006 (2017), <http://dx.doi.org/10.1063/1.4993348>
- <sup>16</sup> M. K. M. Haafiz, A. Hassan, R. Arjmandi, Z. Zakaria, M. M. Marliana *et al.*, *Polym. Polym. Compos.*, **24**, 675 (2016), <https://doi.org/10.1177/096739111602400901>
- <sup>17</sup> C. P. Azubuike, J. O. Odulaja and A. O. Okhamafe, *J. Excipients Food Chem.*, **3**, 106 (2012)
- <sup>18</sup> C. P. Azubuike and A. O. Okhamafe, *J. Recycl. Org. Waste Agric.*, **1**, 1 (2012)
- <sup>19</sup> N. A. Bhimte and P.T. Tayade, *AAPS J.*, **8**, 1 (2007), <http://www.aapspharmscitech.org>
- <sup>20</sup> Y. P. Chauhan, R. S. Sapkal, V. S. Sapkal and G. S. Zamre, *Int. J. Chem. Sci.*, **7**, 681 (2009), <http://www.ncbi.nlm.nih.gov/pubmed/19107185>
- <sup>21</sup> K. Bhandari, A. Adaval, A. R. Bhattacharyya and A. R. Maulik, *J. Nat. Fibers*, **19**, 1 (2020), <https://doi.org/10.1080/15440478.2020.1788688>
- <sup>22</sup> M. Beroual, D. Trache, O. Mehelli, L. Boumaza, A. F. Tarchoun *et al.*, *Waste Biomass Valoriz.*, **12**, 2779 (2021), <https://doi.org/10.1007/s12649-020-01198-9>
- <sup>23</sup> M. Beroual and O. Mehelli, in "Materials Research and Applications Part of Materials Horizons: From Nature to Nanomaterials", edited by D. Trache, L.

- Boumaza and A. F. Tarchoun, 2020, pp. 978-981
- <sup>24</sup> D. Trache, M. H. Hussin, C. T. H. Chuin, S. Sabar, M. R. Fazita *et al.*, *Int. J. Biol. Macromol.*, **93**, 789 (2016), <https://doi.org/10.1016/j.ijbiomac.2016.09.056>
- <sup>25</sup> K. Das, D. Ray, N. R. Bandyopadhyay and S. Sengupta, *J. Polym. Environ.*, **18**, 355 (2010), <https://doi.org/10.1007/s10924-010-0167-2>
- <sup>26</sup> C. Sun, *J. Pharm. Sci.*, **94**, 2132 (2005), <https://doi.org/10.1002/jps.20459>
- <sup>27</sup> W. J. Sun and C. C. Sun, *Int. J. Pharmaceut.*, **585**, 119517 (2020), <https://doi.org/10.1016/j.ijpharm.2020.119517>
- <sup>28</sup> J. Chen, X. Wang, Z. Long, S. Wang, J. Zhang *et al.*, *Int. J. Biol. Macromol.*, **165**, 2295 (2020), <https://doi.org/10.1016/j.ijbiomac.2020.10.117>
- <sup>29</sup> S. Sakuri, D. Ariawan and E. Surojo, *AIP Conf. Proc.*, **209**, 7 (2019), <https://doi.org/10.1063/1.5098240>
- <sup>30</sup> M. El-Sakhawy and M. L. Hassan, *Carbohydr. Polym.*, **67**, 1 (2007), <https://doi.org/10.1016/j.carbpol.2006.04.009>
- <sup>31</sup> A. D. Fernadopulle, L. Karunanayake, D. A. S. Amarasinghe, A. M. P. B. Samarasekara and D. Attygalle, *Cellulose Chem. Technol.*, **55**, 469 (2021), <https://doi.org/10.35812/CelluloseChemTechnol.2021.55.43>
- <sup>32</sup> D. Kundu and T. Banerjee, *Heliyon*, **6**, e03027 (2020), <https://doi.org/10.1016/j.heliyon.2019.e03027>
- <sup>33</sup> A. Zyane, E. A. Houssaine, E. M. Sabbar, F. Brouillette and A. Belfkira, *Heliyon*, **6**, e04977 (2020), <https://doi.org/10.1016/j.heliyon.2020.e04977>
- <sup>34</sup> M. Li, B. He and L. Zhao, *BioResources*, **14**, 3231 (2019), <https://doi.org/10.15376/biores.14.2.3231-3246>
- <sup>35</sup> Y. Kai, J. I. Hamada, M. Morioka, T. Todaka, S. Hasegawa *et al.*, *Am. J. Neuroradiol.*, **21**, 1160 (2000)
- <sup>36</sup> D. Trache, M. H. Hussin, C. T. H. Chuin, S. Sabar, M. R. N. Fazita *et al.*, *Int. J. Biol. Macromol.*, **93**, 789 (2016), <https://doi.org/10.1016/j.ijbiomac.2016.09.056>
- <sup>37</sup> M. Rasheed, M. Jawaid, Z. Karim and L. C. Abdullah, *Molecules*, **25**, 122824 (2020), <https://doi.org/10.3390/molecules25122824>
- <sup>38</sup> K. Kitano, S. Hamaguchi, Patent Application Publication, Pub. No.: US 2010/0292345 A1, 2010, <https://patentimages.storage.googleapis.com/3b/c9/82/c2/83c7b24afe69/US20100019677A1.pdf>
- <sup>39</sup> S. Park, J. O. Baker, M. E. Himmel, P. A. Parilla and D. K. Johnson, *Biotechnol. Biofuels*, **3**, 10 (2010), <https://doi.org/10.1186/1754-6834-3-10>
- <sup>40</sup> J. T. Oberlerchner, T. Rosena and A. Potthast, *Molecules*, **20**, 10313 (2015), <https://doi.org/10.3390/molecules200610313>
- <sup>41</sup> M. Poletto, V. Pistor, M. Zeni and A. J. Zattera, *Polym. Degrad. Stabil.*, **96**, 679 (2011), <https://doi.org/10.1016/j.polymdegradstab.2010.12.007>
- <sup>42</sup> V. Hospodarova, E. Singovszka and N. Stevulova, *Am. J. Anal. Chem.*, **09**, 303 (2018), <https://doi.org/10.4236/ajac.2018.96023>
- <sup>43</sup> M. Tyufekchiev, A. Kolodziejczak, P. Duan, M. Foston, K. Schmidt-Rohr *et al.*, *Green Chem.*, **21**, 5541 (2019), <https://doi.org/10.1039/C9GC02466B>
- <sup>44</sup> M. Kaur, S. Kumari and P. Sharma, *Adv. Res.*, **13**, 1 (2018), <https://doi.org/10.9734/AIR/2018/38934>
- <sup>45</sup> M. T. Arowona, G. A. Olatunji, O. D. Saliu, O. R. Adeniyi, O. Atolani *et al.*, *J. Turk. Chem. Soc. A: Chem.*, **5**, 1177 (2018), <https://doi.org/10.18596/jotcsa.327665>
- <sup>46</sup> S. Ardizzone, F. S. Dioguardi, T. Mussini, P. R. Mussini, S. Rondinini *et al.*, *Cellulose*, **6**, 57 (1999), <https://doi.org/10.1023/A:1009204309120>
- <sup>47</sup> D. F. Steele, R. C. Moreton, J. N. Staniforth, P. M. Young, M. J. Tobyn *et al.*, *AAPS J.*, **10**, 494 (2008), <https://doi.org/10.1208/s12248-008-9057-0>
- <sup>48</sup> K. B. Tan, A. Z. Abdullah, B. A. Horri and B. Salamatinia, *J. Chem. Soc. Pakistan*, **38**, 651 (2016), <https://openresearch.surrey.ac.uk/esploro/outputs/journalArticle/Adsorption-Mechanism-of-Microcrystalline-Cellulose-as/99511965002346#file-0>